https://cejsr.academicjournal.io

Synthesis of Polycrystalline $Zn_xcd_{1-X}te$ Solid Solution Films by the Gas Transport Method in a Hydrogen Flow

Sh. B. Utamuradova, S. A. Muzafarova
Institute of Semiconductor Physics and Microelectronics at the National University of Uzbekistan

B. U. Imomov
Samarkand State Architectural and Building Institute

ABSTRACT

The effect of ultrasonic treatment on the generation characteristics of ¬the interface between the SDS of CdTe / CTO structures obtained by magnetron ion sputtering has been studied. It is shown that ultrasonic treatment leads to a decrease in the surface generation rate and an increase in the generation lifetime of minority charge carriers. The observed effects are related to the rearrangement of the defective structure of the transition ¬layer at the interface CdTe / TeO 2 and adjacent CdTe region in the SDS structure CdTe / CTO .

KEYWORDS: *Oxide, film, ultrasound, ¬no equilibrium, oxygen, defect ,semiconductor* structures.

Introduction. Among the A2B6 substances with n-type and p-type conductivity are cadmium and zinc tellurides. In all composition ranges, ZnTe and CdTe compounds produce a continuous solid solution. [1; C.65-95. 2; C.1362-1364]. The kind of conductivity and the photosensitivity in the spectrum of light radiation vary as the composition x of the $Zn_xCd_{1-x}Te$ compound changes. According to the solid solution's composition, [7] reports on the development of effective film photodetectors with maximal spectral photosensitivity in the spectral region of 280–480 nm. Such photodetectors have a photosensitivity spectrum that is solely dependent on the manufacturing method and source material's makeup. A group of photodetectors sensitive in various spectral areas is required to operate in a broad spectral range of light radiation. This makes photodetectors with a spectrally dependent parameter and an operationally configurable photosensitivity spectrum that are affected by an external factor, such an applied mixing voltage, very interesting.

To achieve this, it is imperative to thoroughly examine the technological underpinnings of the creation of large-block polycrystalline films based on wide-gap semiconductors, particularly based on A^2B^6 semiconductor compounds, which are, in turn, not inferior to single crystals of ZnCdTe compounds due to their wide band gap and high photosensitivity. Since films of the $Zn_xCd_{1-x}Te$ solid solution have excellent photosensitivity and have a high internal quantum yield in the intrinsic absorption region, they were chosen as the basic material for the construction of X-ray and γ -radiation photodetectors based on polycrystalline $Zn_xCd_{1-x}Te$. One may easily change the band gap as well as the characteristics of the grain surface and grain boundaries by altering the amount of Zn atoms (x1) in the material. As a result, additional technical study focused on developing solid solution films appropriate for building effective diode structures based on polycrystalline $Zn_xCd_{1-x}Te$ for constructing X-ray and γ -radiation detectors with a regulated spectrum.

Experiment. By adjusting the vapor pressure of the necessary component and, consequently, the evaporation rate, it is possible to alter the composition of the growing film when utilizing the gas transport reaction technique in a hydrogen flow.

A quasi-closed volume is housed inside of a sealed quartz reactor in a system that permits the application of the gas transport reaction technique. A resistive furnace with a specific temperature gradient is moved along its length to regulate the temperature in the source and substrate zones. Chromel - aluminum thermocouples are used to regulate the temperature in the zones. Through tubes that have a distributor, the transport gas (hydrogen) is introduced into the system.

Studies have been done on the relationships between the growth rate of $Zn_xCd_{1-x}Te$ films and the flow rate of hydrogen H_2 and the substrate temperature T_p. The setup for developing the $Zn_xCd_{1-x}Te$ solid solution is shown in Fig. 1. The temperatures of the source and substrate during layer deposition were measured with chromel-alumel thermocouples.

Several technical processes work in tandem to carry out the evaporation process in the system [3; C.231-235; four; C.411-416; five; C.314-318]. A quartz glass is inserted in the upper portion of the reactor to hold the substrate, and the installation includes two crucibles for CdTe and ZnTe. A water-cooled flange (1) holds the quartz tube reactor (3) in place, and glands are used to seal the reactor (2). The exterior portion of the reactor is firmly fastened using a slip-on flange. A branch pipe in the center of the reactor is used to provide the carrier gas H_2, and a branch pipe in the bottom portion of the cooled flange is used to discharge it. The quartz stand (4) and graphite adapter are joined by the quartz glass (11). (8). On the glass, a substrate holder (12) is positioned (11). A thermocouple (6) within a mobile quartz tube (7) fastened to the flange with glands measures the substrate temperature T_p. The quartz tube (7) also serves as the substrate fixer at the same time. The heat source for the reactor is a detachable two-probe furnace (5).

In addition, the lower electrical contact to the base layer of the developed structure was made using a molybdenum substrate with a thickness of ~100 mkm. The high melting point, chemical inertness, thermal stability, and ohmic contact to a solid solution of molybdenum are reasons for its selection.

Molybdenum was used as a substrate for the semiconductor solid solution $Zn_xCd_{1-x}Te$ synthesis. Molybdenum was first oxidized in nitric acid HNO3, the oxide was then removed in HF, and finally the substrate was washed in distilled water.

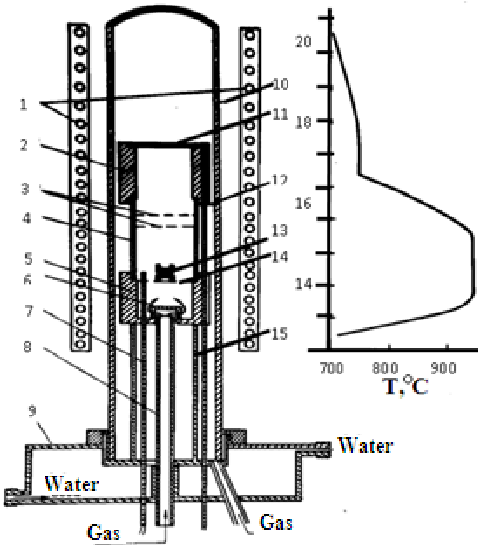

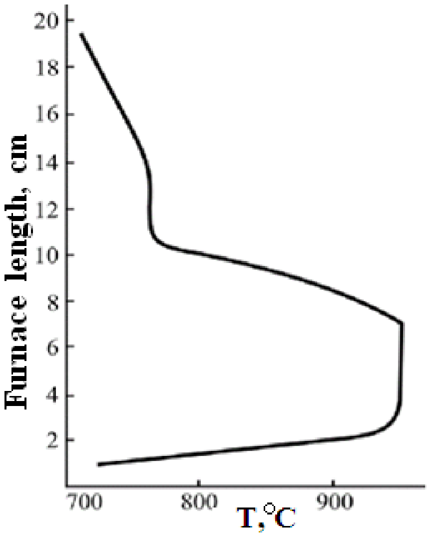

Fig. 1 Installation for growing $Zn_xCd_{1-x}Te$ films in H_2 flow.

Fig.2. the temperature gradient of a two-probe furnace for synthesis of films $Zn_xCd_{1-x}Te$

The optimal T_{CdTe} source temperature was T_i=950^{0}C, the optimal T_{ZnTe} source temperature was

$T_i=1100^0$C, and the substrate temperature $T_p \approx 650^0$C. The rate of the inert gas, hydrogen, was υ =1.5–1.9 l/h.

The quasi-closed volume within the reactor ensures the production of the necessary vapor pressure of the ZnTe and CdTe components close to the substrate, increasing the rate of film growth and decreasing the consumption of the initial material, which results in the formation of $Zn_xCd_{1-x}Te$ layers with a consistent surface area and thickness.

In the process of film deposition under the optimal mode, the film growth rate was 100÷300 Å/sec. At the evaporation temperature Ti=9500C for CdTe and Ti=11000C for ZnTe, the compounds pass into the vapor phase,

$$CdTe_T + H_2 \leftrightarrows CdTe_п + H_2, \qquad (1)$$

$$ZnTe_T + H_2 \leftrightarrows ZnTe_п + H_2. \qquad (2)$$

Then, in the vapor phase, CdTe and ZnTe dissociate into cadmium, zinc, and tellurium,

$$2CdTe_п + H_2 \leftrightarrows 2Cd_п + Te_{2п} + H_2, \qquad K = \frac{P_{Cd}^2 \cdot P_{Te_2}}{P_{CdTe}^2}, \qquad (3)$$

$$2ZnTe_п + H_2 \leftrightarrows 2Zn_п + Te_{2п} + H_2, \qquad K = \frac{P_{Zn}^2 \cdot P_{Te_2}}{P_{ZnTe}^2}. \qquad (4)$$

The released vaporous tellurium reacts with hydrogen and forms hydrogen telluride.

$$Te_{2п} + 2H_2 \leftrightarrows 2H_2Te, \quad K = \frac{P_{H_2Te}^2}{P_{Te_2}}. \qquad (5)$$

Vaporous CdTe and ZnTe cannot completely dissociate, and then

$$CdTe_п + H_2 \leftrightarrows Cd_п + H_2Te, \qquad K = \frac{P_{Cd} \cdot P_{H_2Te}}{P_{CdTe}}, \qquad (6)$$

$$ZnTe_п + H_2 \leftrightarrows Zn_п + H_2Te, \qquad K = \frac{P_{Zn} \cdot P_{H_2Te}}{P_{ZnTe}}, \qquad (7)$$

$$Te_{2п} = 2Te_п, \qquad K = \frac{P_{Te}^2}{P_{Te_2}}. \qquad (8)$$

On the substrate surface, reaction (5) proceeds in the opposite direction, and as a result of the interaction of cadmium, zinc, and tellurium atoms, a $Zn_xCd_{1-x}Te$ film is formed on the substrate.

$$xZn_п + (1 - x)_п + H_2Te \rightarrow Zn_xCd_{1-x}Te + H_2, \qquad (9)$$

$$K = (PZnx \cdot PCd1{-}x \cdot PH2Te){-}1.$$

The composition of the films x depends on the ratio of the components of the vapor phase mixture, which is determined by the rate of evaporation of the CdTe and ZnTe sources. At *x*=0, equation (9) will take the form

$$Cd_п + H_2Te \rightarrow CdTe_т + H_2, \quad K = (P_{Cd} \cdot P_{H_2Te})^{-1}, \qquad (10)$$

and at *x* =1

$$Zn_п + H_2Te \rightarrow ZnTe_т + H_2, \quad K = (P_{Zn} \cdot P_{H2}Te)^{-1}. \qquad (11)$$

Temperatures TCdTe and TZnTe are set in such a way that complete evaporation of CdTe and ZnTe powders is ensured. The composition of the CdTe - ZnTe film was varied by changing the ratio of the weight parts of the loaded powders in the crucibles. With this in mind, the chemical composition of the $Zn_xCd_{1-x}S$ films was determined at first only depending on the temperature of the ZnS and CdS sources at constant T_p=650 °C and V_{gas}=1.5 l/h (sm Table 1).

Table1.

Sample	Source temperature ZnTe, ^oC	Source temperature CdTe,^oC	Substrate temperature ^oC	Hydrogen speed л/ч
1	1050÷1100	700÷750	650	1,5
2	950÷1000	800÷850	650	1,5

At a carrier gas flow of υ =1.5–1.9 l/h, Figure 2 illustrates the temperature dependence of the rate of evaporation of powders from CdTe and ZnTe crucibles. According to the slope of the direct dependency (Fig. 2), the activation energy and evaporation rates for CdTe and ZnTe were 45 and 50 kcal/mol, respectively. These values are in good agreement with the heat of evaporation for these two materials. [6; C.310].

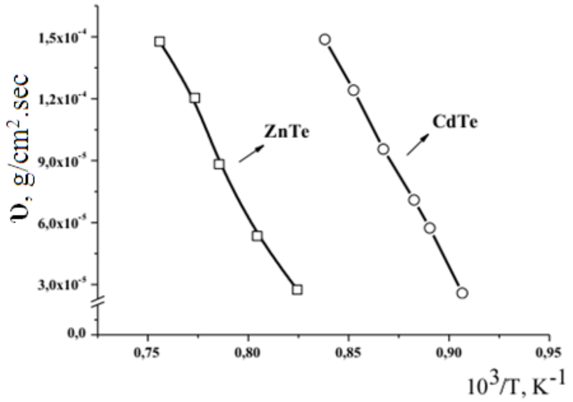

Fig.2. Temperature dependence of the evaporation rate of powders

CdTe and ZnTe from crucibles, carrier gas flow υ=1.5÷1.9 л/час.

Figure 3 shows the dependence of the Zn_xCd_1xTe film growth rate on the carrier gas flow at source temperatures TCdTe=1175 K and TZnTe=1328 K, respectively. It can be seen from this dependence that the thickness of the Zn_xCd_1xTe film reaches its highest value at a flow of carrier gas (hydrogen) υ = 1.5 l/h and has a maximum value (d ≈ 70÷80 мкм/час).

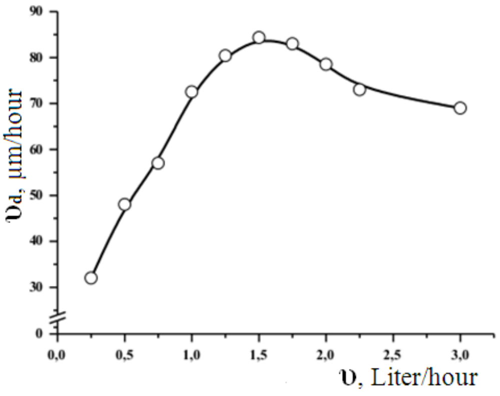

Fig.3. Dependence of the $Zn_xCd_{1-x}Te$ film growth rate on the carrier gas flow, at TCdTe=1175 K, TZnTe=1328 K.

The thickness of the $Zn_xCd_{1-x}Te$ films was determined on an MII-4 microinterferometer. Separating the film from the molybdenum substrate by weighing method, the film thickness d is calculated by the formula

$$d = \frac{m}{\rho S}$$

here, ρ – density of the condensing substance, S – grown layer area, m – film weight.

It should be noted that the thickness of $Zn_xCd_{1-x}Te$ films can be varied at given technological parameters by changing the growth time.

In Fig.4. the dependence of the growth rate of $Zn_xCd_{1-x}Te$ films on the substrate temperature, the temperature of the evaporators TCdTe and TZnTe is shown. As can be seen from Fig. 4, at low and high substrate temperatures, the thicknesses of the synthesized films have low values, which are due to the fact that at lower substrate temperatures, fine-grained and thin layers are formed, and at high substrate temperatures, particle reevaporation from the film surface is observed.

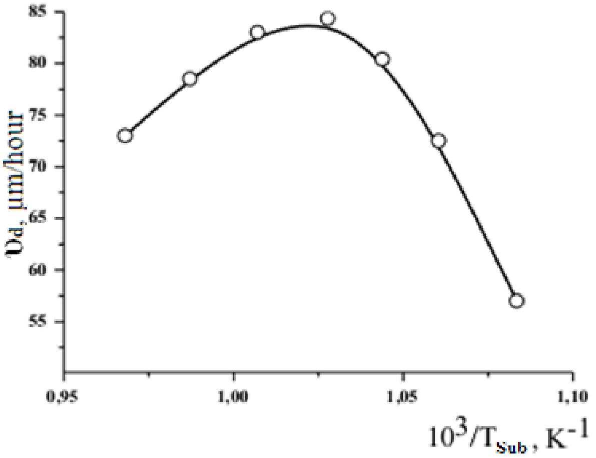

Fig.4. Dependence of the $Zn_xCd_{1-x}Te$ film growth rate on the substrate temperature, TCdTe=1178 K, and TZnTe=1328 K and v=1.5 l/h.

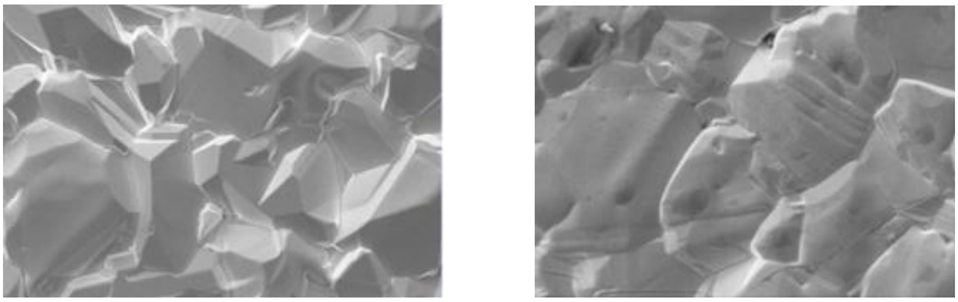

(a) **(b)**

Fig5. Surface microstructure of $Zn_xCd_{1-x}Te$ films synthesized at different substrate temperatures: a) T_p=650^{0}C, b) T_p= 750^{0}C .

Figure 5 shows the microstructure of the surface of $Zn_xCd_{1-x}Te$ film samples synthesized at substrate temperatures of 650^{0}C and 750^{0}C by the method of scanning electron microscopy on a setup (Scanning electron microscope) SEM- EVO MA 10 - CARL ZEISS.

The analysis of the film's morphological characteristics, including grain sizes and thicknesses, in relation to technical factors revealed that the source temperatures (TCdTe and ZnTe), substrate temperature (T_p), and carrier gas flow (υ) had the most effects on the morphology. A thick, coarsegrained $Zn_xCd_{1-x}Te$ layer develops under these circumstances.

The analysis of microstructures (Fig. 5) shows that with an increase in the temperature of the Mo substrate to 750 ^oC, the grain sizes increase, the disorientation of crystallites disappears, and a polycrystalline film with densely packed crystallites is formed by oriented grains. The results of the study of the influence of the substrate temperature on the chemical composition of $Zn_xCd_{1-x}Te$ films in the range T_p=550÷650 °C are presented in Table 2 $Zn_xCd_{1-x}Te$

Table 2

Substrate temperature ^oC	The content of zinc in the film $Zn_xCd_{1-x}Te$	Lattice parameters, Å
550	0,1	4,08
580	0,15÷0,2	4,018
600	0,3÷0,35	3,98
620	0,4	3,93
650	0,5	3,09

Table 2 shows that the zinc concentration of the solid solution increases as T_p increases. The crystal lattice parameter also rises as a result. This situation shows a satisfactory agreement with Vegard's law [8], which validates the films' stoichiometry.

Only a hexagonal wurtzite-type phase was found when the phase composition of $Zn_xCd_{1-x}Te$ films was studied along the thickness using layer-by-layer etching in a 25% solution at 60°C. The thickness-dependent constant function of film composition. The best technical regime may be identified thanks to these experimental findings in order to produce $Zn_xCd_{1-x}Te$ films with the best structural characteristics.

As a result, a technique has been created for producing $Zn_xCd_{1-x}Te$ films with the best structural characteristics.

The quantity of expanded grain boundaries grows at the same time that homogenization takes place. Based on the results, it can be inferred that the ideal temperature range for the substrate during the synthesis of $Zn_xCd_{1-x}Te$ films should be 650°C. At temperatures of 650°C, the crystallite size equates to 15÷45 m, whereas at 750°C, the crystallite size ranges from 30÷70 m.

The resistivity at substrate temperatures of 650°C and 750°C was ρ = 3.3 105 Ω cm and ρ = 1.87 105 Ω cm, respectively.

As a result, the $Zn_xCd_{1-x}Te$ films produced using the hydrogen flow technique of gas transport have relatively acceptable morphological features and are produced using the following technological parameters: Temperatures of the substrate are T_p = 650^0C, the evaporator is Ti=10500C (ZnTe), and Ti=900^0C. (CdTe). In this instance, the growth rate was calculated to υ = 80–85 m/h. The films had a specific resistance value of ρ = 10^4 Om·cm at room temperature and had a grain size of 30÷70 mkm. The $Zn_xCd_{1-x}Te$ materials optical and electrophysical characteristics are primarily influenced by technical growth regimes, with the composition of the $Zn_xCd_{1-x}Te$ solid solution compound changing as a contributing factor.

References

1. Физика и химия соединений A^2B^6. Под ред. проф. С.А. Медведова, −М.:

   Мир. –1970. − С. 65-95.

2. Shukla A.K., Pathak H.P., Sharma S.K., Dwivedi D.K. Morphological study of

   $Zn_xCd_{1-x}Te$ thin films // Imperial journal of interdisciplinary research (IJIR).

– 2017. Vol. 5, Iss. 5. − pp.1362-1364.

3. Mirsagatov Sh.A., Makhmudov M.A., Ataboev O.K., Ataboeva F.K. Influence of Ultrasonic Irradiation on the Output Parameters of Photosensitive In-n^+CdSnCdS$_x$Te$_{1-x}$-pZn$_x$Cd$_{1-x}$Te-Mo Heterostructure // Applied Solar Energy. –2016. Vol. 52. №3. − pp. 231-235.
4. Razykov T.M., Kuchkarov K.M., Ferekides C.S., Ergashev B.A., Yuldoshov R.T., Mamarasulov N.K., Zufarov M.A. Characterization of CdTe thin films with different compositions obtained by CMBD for thin film solar cells // Solar energy. 2017. Vol. 144. − pp. 411-416.
5. Kuchkarov K.M., Razykov T.M., Ferekides C.S., Ergashev B.A., Yuldoshov R.T., Zufarov M.A. Research of the morphological and structural properties of CdTe films obtained by Chemical molecular beam deposition for thin film solar cells // Applied solar energy. 2015. Vol. 51. №4. − pp. 314-318.
6. Калинкин И. П., Алесковский В. Б., Симашкевич А. В. Эпитаксиальные пленки соединений A2B6. −Л.: Изд-во Ленингр. Ун-та, 1978. – С.310
7. Тонкие полукристаллические и аморфные пленки. Под ред. Л.Каземерски «Мир» 1983.
8. A. R. Denton and N. W. Ashcroft. Vegard’s law. Phys. Rev. A, 43:– pp.3161–3164, March 1991.
9. Nabievich, M. M., & Kholikovich, R. K. The Importance and Role of" Safety of Life Activities" Subject in Higher Educational Institutions. JournalNX, 9-13.
10. Rakhmonberdievich, Y. O., & Razzokov, K. K. (2022). Scientific Methods of Optimization of Labor Safety in Economic Sectors. European Journal of Life Safety and Stability (2660-9630), 232-237.